# STEADY DIFFUSION-DRIVEN FLOW IN A TILTED SQUARE CONTAINER

*by* MICHAEL A. PAGE

(*School of Mathematical Sciences, Monash University, Clayton, Victoria* 3800*, Australia*)

[Received 20 November 2010, Revised 5 April 2011]

**Summary**

This paper considers 'diffusion-driven flows', for which a temperature flux condition on a sloping non-slip surface in a stratified fluid generates a slow steady upward flow along a thin 'buoyancy layer'. The principles for this steady-flow phenomenon are well-understood in a semi-infinite fluid and more recently have been applied to steady flows within a contained fluid under more general conditions, including where buoyancy layers expel or entrain fluid from their outer edge. In this paper additional features of these flows are described in the context of a two-dimensional flow in a tilted square box, and some of the finer details of flow structure are elucidated. In particular, the key regions of the asymptotic structure are considered when the Wunsch-Phillips parameter $R$ is small, and the leading-order solutions are derived in most of those regions. To illustrate the theory, three simple case studies of diffusion-driven motion are solved, and the results compared with accurate numerical solutions for $R = 10^{-4}$. In some cases a 'corner-induced' motion is found to occur, extending across the width of the container. The details of that feature are examined using both higher-order solutions of the outer flow and an integral treatment across the corner regions, and a solution for the corresponding '$R^{1/3}$-layer flow' is proposed. Theoretical and numerical results are compared as the angle of inclination $\beta$ is varied.

**Q. Jl Mech. Appl. Math. (2011) 64 (doi:10.1093/qjmam/hbr007), 1–5** 

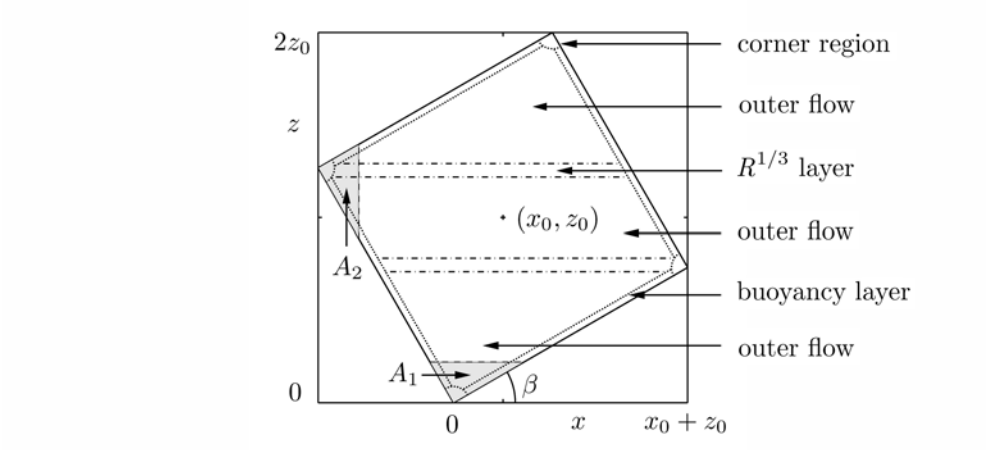


**Fig. 1** Geometry of the tilted-square configuration considered in §3, in §4 when $\beta = \pi/4$ and in §6 for $0 < \beta < \pi/2$.

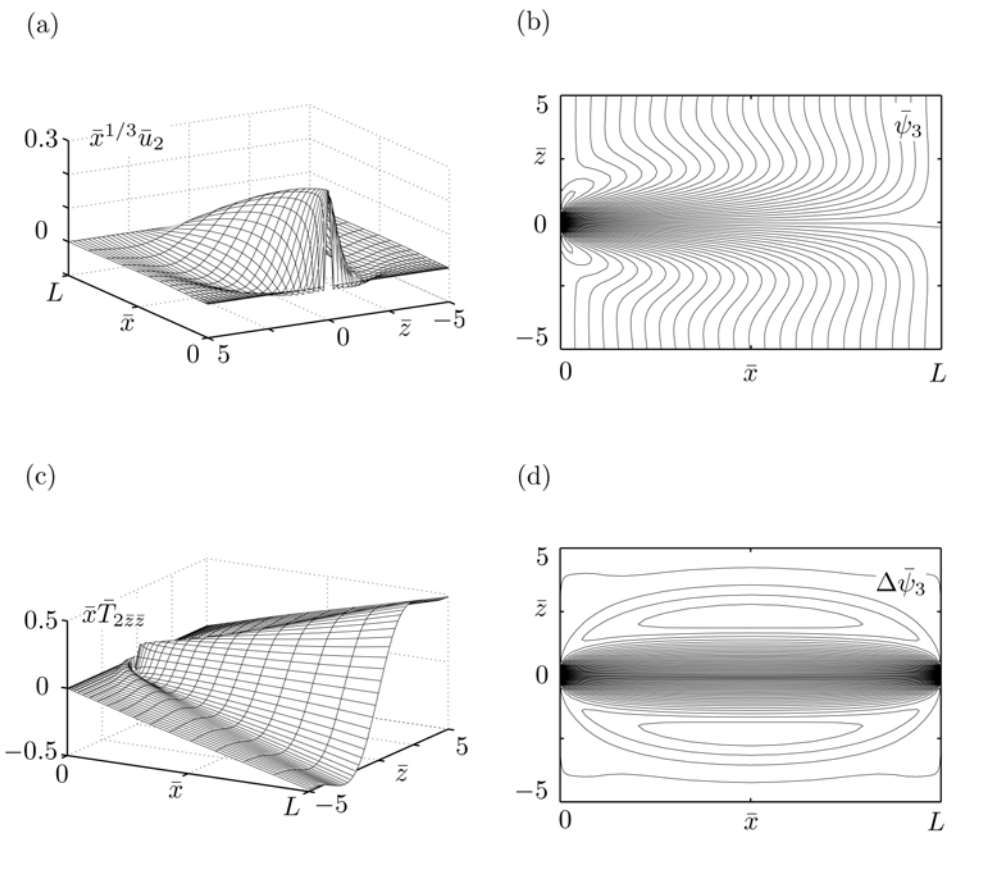


**Fig. 2** Plots of the $R^{1/3}$-layer solution when $\mu = 1$ and $L = 1$ for (a) the 'jet' velocity $\bar{x}^{1/3}\bar{u}_2(\bar{x}, \bar{z})$ based on the solution (3.18); (b) the corresponding streamlines of $\bar{\psi}_3(\bar{x}, \bar{z})$; (c) the scaled second derivative $\bar{x}\bar{T}_{2\bar{z}\bar{z}}(\bar{x}, \bar{z})$ from (3.18), showing that $\bar{T}_{2\bar{z}\bar{z}}$ resolves a discontinuity of $T_0''$ across the $R^{1/3}$ layer; (d) streamlines of $\Delta\bar{\psi}_3(\bar{x}, \bar{z}) = [\bar{\psi}_3(\bar{x}, \bar{z}) - \bar{\psi}_3(L - \bar{x}, -\bar{z})]$, corresponding to a unit source at $\bar{x} = 0$ and unit sink at $\bar{x} = L$.

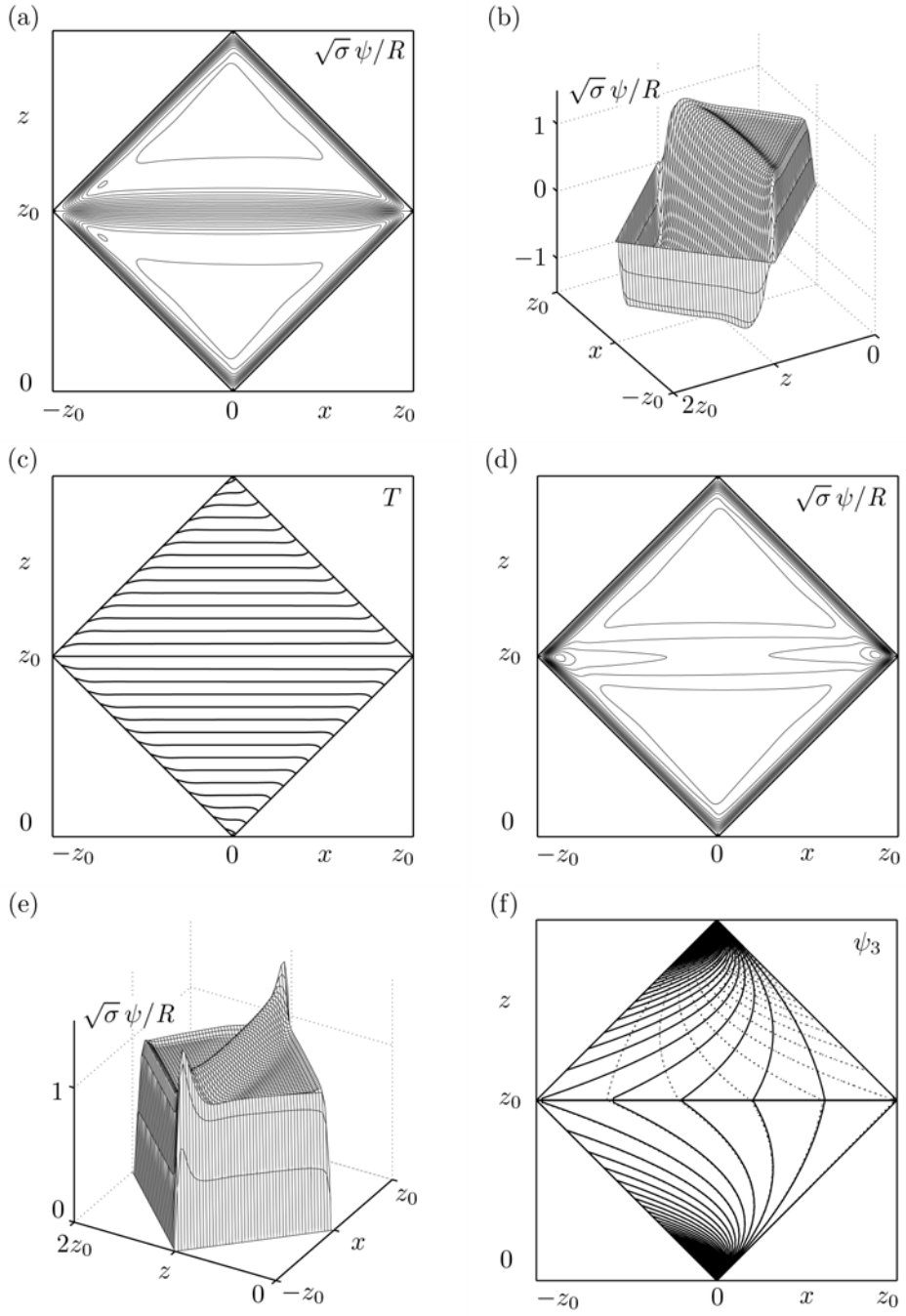


**Fig. 3** Numerical solutions of the full equations for $R = 10^{-4}$, $\epsilon = 1$ and $\sigma = 1$. (a) Streamlines for Case 1a; (b) plot of $\sqrt{\sigma}\,\psi/R$ for Case 1a; (c) contour plot of the corresponding temperature $T$; (d) streamlines for Case 1b; (e) plot of $\sqrt{\sigma}\,\psi/R$ for Case 1b; (f) streamlines for the higher-order streamfunction $\psi_3$ in the outer flow for Case 1a (unbroken lines) and Case 1b (dotted lines).

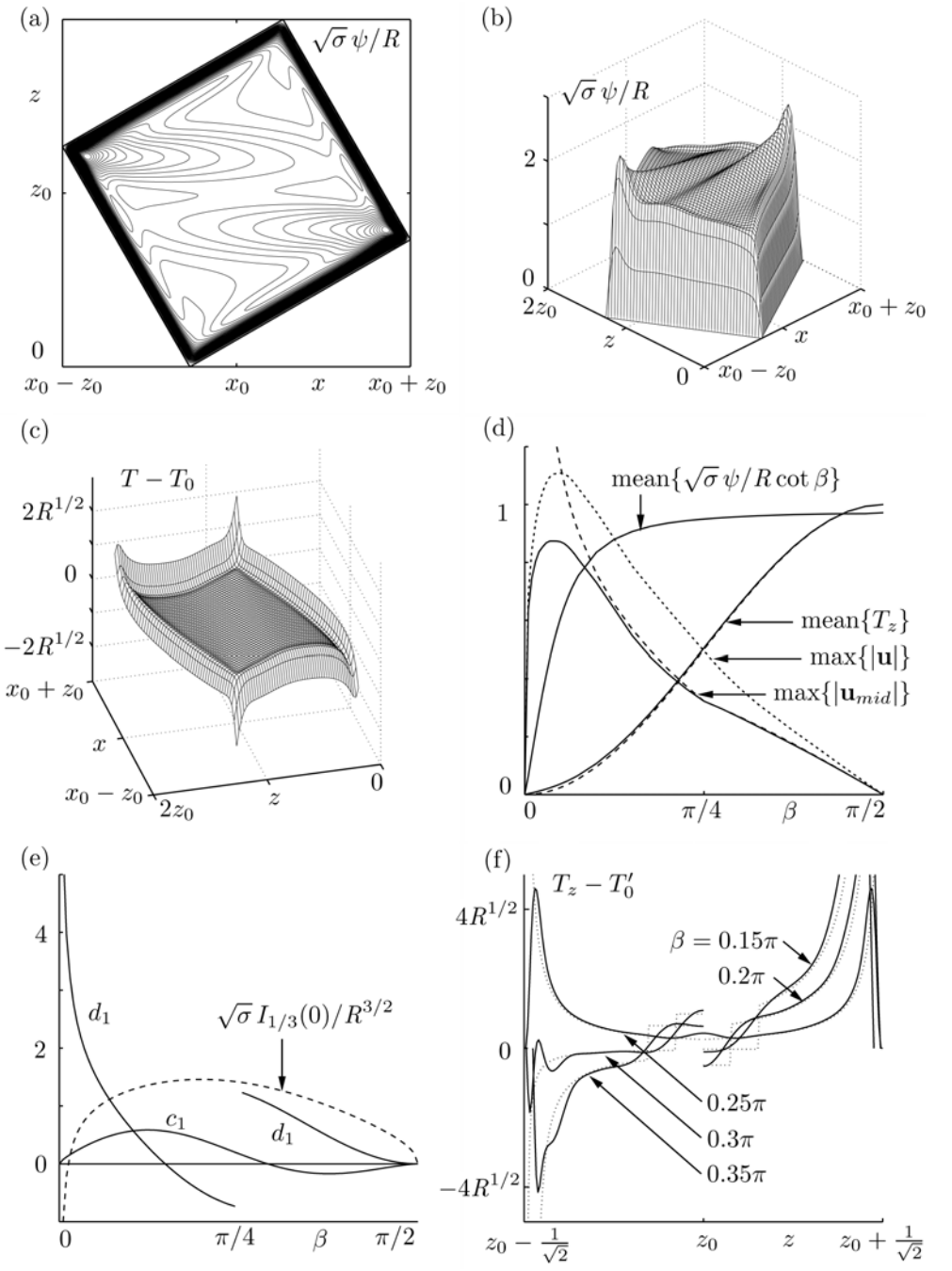


**Fig. 4** Numerical solutions for Case 2 when $R = 10^{-4}$ and $\sigma = 1$. (a) Streamlines when $\beta = \pi/6$; (b) plot of $\sqrt{\sigma}\,\psi/R$; (c) plot of $[T - T_0]$; (d) maximum velocity $\max\{|\mathbf{u}|\}$, 'mid-sectional' maximum $\max\{|\mathbf{u}_{mid}|\}$ and mean values of $(\sqrt{\sigma}\,\psi/R\cot\beta)$ and $T_z$, showing estimated values (dashed lines); (e) plots of $c_1$, $d_1$ and $\sqrt{\sigma}\,I_{1/3}(0)/R^{3/2}$ (dashed line) from §6.6; (f) cross-section of $[T_z - T_0']$ compared to $T_1'(z)$ (dotted lines) when $\beta/\pi = 0.15, 0.2, 0.25, 0.3$ and $0.35$.

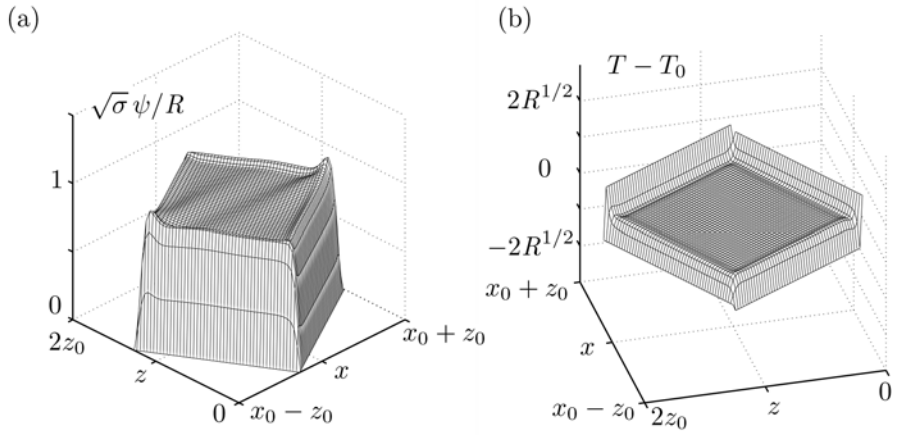


**Fig. 5** Numerical solutions of the full equations for Case 3 when $R = 10^{-4}$ and $\sigma = 1$. (a) Plot of the streamfunction $\sqrt{\sigma}\,\psi/R$ when $\beta = \pi/6$; (b) plot of $[T - T_0]$. Both are to the same scale as on Figs. 4(b)-(c).